

LLM-3D Print: Large Language Models To Monitor and Control 3D Printing

Yayati Jadhav^{1,†}, Peter Pak,[†] and Amir Barati Farimani^{*,†,‡}

[†] *Department of Mechanical Engineering, Carnegie Mellon University, Pittsburgh, PA, USA*

[‡] *Machine Learning Department, Carnegie Mellon University, Pittsburgh, PA, USA*

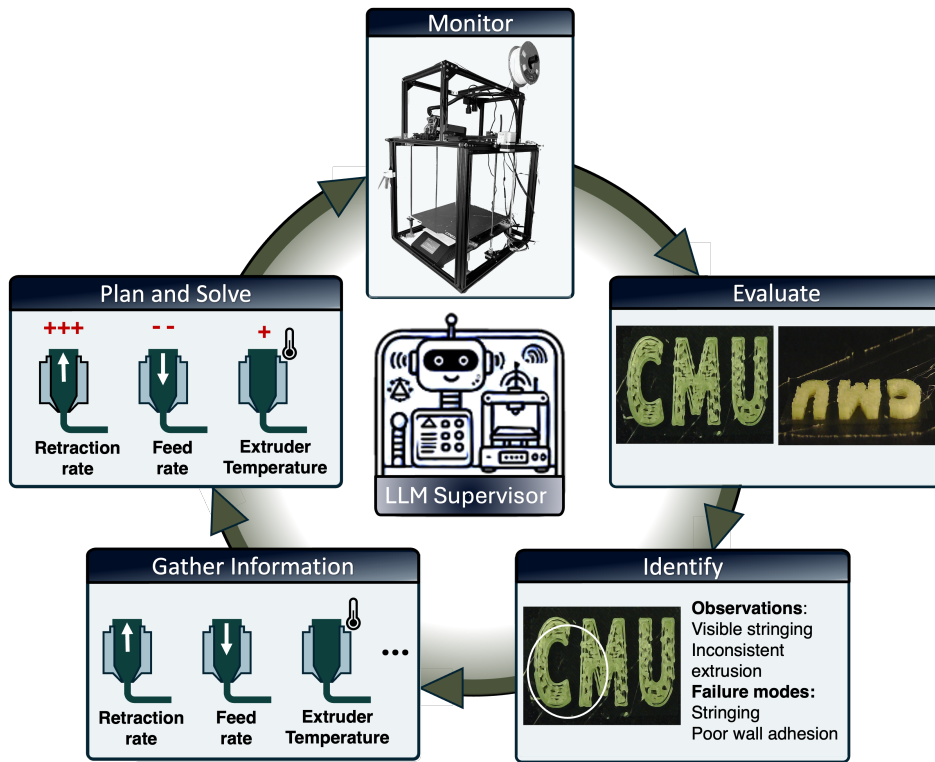
E-mail: barati@cmu.edu

Website: <https://sites.google.com/andrew.cmu.edu/printerchat>

Abstract

Industry 4.0 has revolutionized manufacturing by driving digitalization and shifting the paradigm toward additive manufacturing (AM). Fused Deposition Modeling (FDM), a key AM technology, enables the creation of highly customized, cost-effective products with minimal material waste through layer-by-layer extrusion, posing a significant challenge to traditional subtractive methods. However, the susceptibility of material extrusion techniques to errors often requires expert intervention to detect and mitigate defects that can severely compromise product quality. While automated error detection and machine learning models exist, their generalizability across diverse 3D printer setups, firmware, and sensors is limited, and deep learning methods require extensive labeled datasets, hindering scalability and adaptability. To address these challenges, we present a process monitoring and control framework that leverages pre-trained Large Language Models (LLMs) alongside 3D printers to detect and address printing defects. The LLM evaluates print quality by analyzing images captured after each layer or print segment, identifying failure modes and querying the printer

for relevant parameters. It then generates and executes a corrective action plan. We validated the effectiveness of the proposed framework in identifying defects by comparing it against a control group of engineers with diverse AM expertise. Our evaluation demonstrated that LLM-based agents not only accurately identify common 3D printing errors, such as inconsistent extrusion, stringing, warping, and layer adhesion, but also effectively determine the parameters causing these failures and autonomously correct them without any need for human intervention.



Abstract Figure: LLMs in continuous improvement cycle LLM-based supervisor agents can be employed at each step of the continuous improvement cycle. The cycle involves evaluating print quality, identifying failure modes, gathering relevant information, and planning and solving the issues by adjusting the print parameters, ensuring high-quality defect-free parts.

Introduction

Industry 4.0, also known as the Fourth Industrial Revolution, integrates the Internet of Things (IoT), artificial intelligence, and big data analytics to assist in smart manufacturing where machines and systems seamlessly communicate to optimize production processes.¹⁻³ This technological integration enhances quality control and certification processes via *in-situ* process monitoring utilizing automated data collection to ensure consistent adherence to quality standards.⁴ Automated documentation facilitates comprehensive traceability, simplifies certification, and provides verifiable records that help manufacturers achieve and maintain industry certifications, boosting compliance and customer trust.⁵

Additive Manufacturing (AM) plays a key role in this industrial revolution, enabling rapid prototyping from conceptual design to production level parts through an iterative design process bypassing the constraints of conventional manufacturing processes.⁶ AM significantly reduces production time, enhances design flexibility, lowers costs, minimizes post-processing, and supports multi-material design through a layer-by-layer printing process.⁷ This gives AM a substantial advantage over traditional subtractive manufacturing techniques, such as CNC machining, by offering greater material efficiency and design versatility.⁸ Consequently, AM has shown promising applications in various fields, including healthcare,^{9,10} medical devices,^{11,12} and aerospace,¹³ among others.¹⁴⁻¹⁶

One of the most widely used additive manufacturing processes is Fused Deposition Modeling (FDM). This technique involves extruding thermoplastic filaments through a heated nozzle, which deposits material layer by layer to construct a part from the bottom up.¹⁷ The accessibility and versatility of FDM have fueled the growth of open-source projects like RepRap,^{18,19} democratizing 3D printing technology and enabling individuals, small businesses,²⁰ and research labs^{21,22} to develop and customize hardware, significantly expanding the applications and accessibility of additive manufacturing.

Despite its advantages, FDM is highly susceptible to errors and failures, which limit its consistency and material efficiency. Common issues include warpage, layer misalignment,

under-extrusion, over-extrusion, and stringing, among others.²³⁻²⁷ These issues are further compounded by the lack of standardized hardware, material variations,²⁸ user errors,²⁹ and print process parameters that are not tailored to specific designs,^{30,31} all of which contribute to significant variations in print quality. Studies indicate that 20% of PLA prints fail,³² ABS prints have a material waste rate of 34%,³³ and overall failure rates can reach 41.1%, with human error accounting for 26.3% of these failures.²⁹ These failures not only result in wasted material, energy, and time but also limit the use of AM parts in end-use products, especially in safety-critical applications like medical devices and aerospace components.

Some notable approaches to address these problems involve simulating the 3D printing process and optimizing process parameters specific to each part.^{30,34} While this method can effectively tailor parameters for individual parts, it is computationally expensive and impractical for manufacturing due to the diverse range of parts and the significant time required for simulations. Another approach to solving failures in FDM focuses on its open-loop control system, which lacks real-time feedback and prevents immediate detection and correction of errors. By converting to a closed-loop system, failures can be detected, and print parameters optimized in real-time, addressing issues related to machine variability, user settings, and part-agnostic print parameters.³⁵ This limitation has spurred innovative research into monitoring and improving extrusion-based additive manufacturing methods.³⁶⁻³⁹ Researchers have employed various sensors, including vibration sensors,⁴⁰ acoustic sensors,⁴¹ accelerometers,⁴² piezo sensors,⁴³ and laser scanners⁴⁴ to enhance the detection and correction of errors in real-time. While these sensors can detect real-time anomalies and reduce print failures, many errors remain undetectable, and their high cost and complexity limit their widespread use in 3D printers.⁴⁵

In contrast, camera-based monitoring systems offer a low-cost and easy-to-integrate alternative for identifying surface defects and other visible issues in 3D printing.⁴⁶⁻⁴⁹ Infrared or thermal cameras can detect anomalies not visible to standard visual cameras,^{50,51} and multi-camera setups can reconstruct 3D models of printed parts to check dimensional and

shape accuracy.^{52,53} Due to their cost-effectiveness and simplicity, standard camera systems have seen more widespread adoption. A notable study developed an image-based closed-loop quality control system for fused filament fabrication, implemented by a customized online image acquisition system with a proposed image diagnosis-based feedback quality control method.⁵⁴ While computer vision approaches are promising for targeting specific errors, they often require calibration for each part, printer, and material, making it difficult to create feature extraction algorithms that generalize across different setups. Consequently, these methods typically work with only a single combination of printer, part geometry, material, and printing conditions. Integrating machine learning techniques offers a more flexible and adaptable solution, enabling robust error detection and correction across diverse printing environments.

Machine learning, particularly deep learning techniques, has achieved state-of-the-art performance in various science and engineering applications. These techniques have been successfully applied to surrogate modeling,⁵⁵⁻⁵⁸ generating 3D printable structures,⁵⁹ and predicting failures in 3D printing,⁶⁰⁻⁶² among other areas.^{63,64} These advancements demonstrate the significant potential of machine learning to enhance and innovate within the field of additive manufacturing.

Recent research has leveraged machine learning for error detection in FDM, demonstrating promising results through camera-based monitoring and convolutional neural networks to predict and correct issues such as extrusion rate,⁶⁵ warpage,⁶⁶ surface defects,⁶⁷ and layer defects.⁶⁸ One notable approach aims to generalize the process across different parts, materials, and printing systems by using convolutional neural networks to detect errors and adjust parameters like flow rate, speed, z-offset, and extruder temperature.⁶⁹

However, most methods are limited to addressing errors in a single modality by changing only a few print parameters and have primarily demonstrated correction of the flow rate parameter in a single geometry used for both training and testing. Additionally, some machine learning models require a reference object for comparison, which restricts their

effectiveness for custom parts.⁶⁷ Furthermore, these methods are not capable of real-time correction, meaning that if an error is detected, the part cannot be recovered. Although Brion et al.⁶⁹ addressed this by splitting the toolpath for a layer into smaller segments, optimizing one segment does not necessarily ensure that subsequent segments will also be optimized, especially if their shapes differ significantly.

Moreover, deep learning requires a large labeled dataset, necessitating many prints, which complicates its implementation for error detection due to the high costs and effort needed to generate sufficient training data. Additionally, deep learning models are usually tailored for specific tasks and perform exceptionally well within those domains but often struggle to adapt to different tasks or scenarios. This lack of flexibility, compared to human problem-solving abilities, underscores the challenge of developing a framework that can adapt to various printer setups, detect multiple print defects, and optimize parameters for different parts. Leveraging pre-trained networks could be a potential solution to this problem.

Leveraging transformer architecture^{70,71} and massive datasets,⁷²⁻⁷⁷ Large Language Models (LLMs) have made significant strides in various natural language processing (NLP) tasks, including text generation and following task-specific instructions.^{78,79} Additionally, LLMs have demonstrated emergent reasoning capabilities by interpolating and utilizing their extensive training data, allowing them to make inferences, draw conclusions, and solve problems beyond their explicit programming.^{80,81} Despite the substantial computational resources required for training and fine-tuning LLMs for specific applications, these models have shown an exceptional ability to generalize to new tasks and domains. This remarkable capability is primarily attributed to the in-context learning (ICL) paradigm.⁷² By using minimal natural language prompts and avoiding extensive fine-tuning, LLMs have emerged as effective "few-shot learners",^{82,83} demonstrating proficiency with limited training examples.

The adaptability of Large Language Models (LLMs) to new domains and their ability to learn in context has been transformative across numerous scientific fields. In chemistry, for example, LLMs have autonomously designed, planned, and executed complex experi-

ments.^{84,85} In mathematics and computer science, these models have discovered novel solutions to longstanding problems like the cap set problem and optimized algorithms for challenges such as the bin-packing problem.⁸⁶ Furthermore, LLMs have significantly advanced research in biomedical fields,^{87–89} materials science,^{90,91} and environmental science.⁹² Their impact extends to other scientific domains as well, enhancing understanding and expanding capabilities.^{93–97} Additionally, LLMs have proven to be effective optimizers for foundational problems such as linear regression and the traveling salesman problem, often matching or exceeding the performance of specialized heuristics through straightforward prompting.⁹⁸ This versatility and efficacy underscore the potential of LLMs to drive innovation and efficiency in a wide array of scientific and engineering applications.

In the field of mechanical engineering, fine-tuned Large Language Models (LLMs) have demonstrated exceptional capabilities in advanced tasks such as knowledge retrieval, hypothesis generation, and agent-based modeling. They have played a crucial role in integrating diverse domains through the use of knowledge graphs.^{99,100} Additionally, LLMs excel in various design-related tasks, including sketch similarity analysis, material selection, engineering drawing analysis, CAD generation, and structural optimization.^{101,102} Their ability to seamlessly connect and enhance these tasks highlights their transformative potential in mechanical engineering.

In this study, we introduce a framework that leverages the multimodal capabilities and emergent reasoning capabilities of LLMs to detect and resolve issues during 3D printing. This framework employs specialized LLM agents assigned to specific tasks, coordinated by a supervisory LLM to ensure efficient workflow and communication. By leveraging the strengths of LLMs in reasoning and optimization, the system identifies errors, qualitatively assesses print quality, gathers necessary information, and addresses these issues. This approach allows for the correction of errors in subsequent layers without discarding the entire part, thereby improving efficiency and reducing material waste.

The hierarchical machine-to-machine framework operates by capturing two images of the

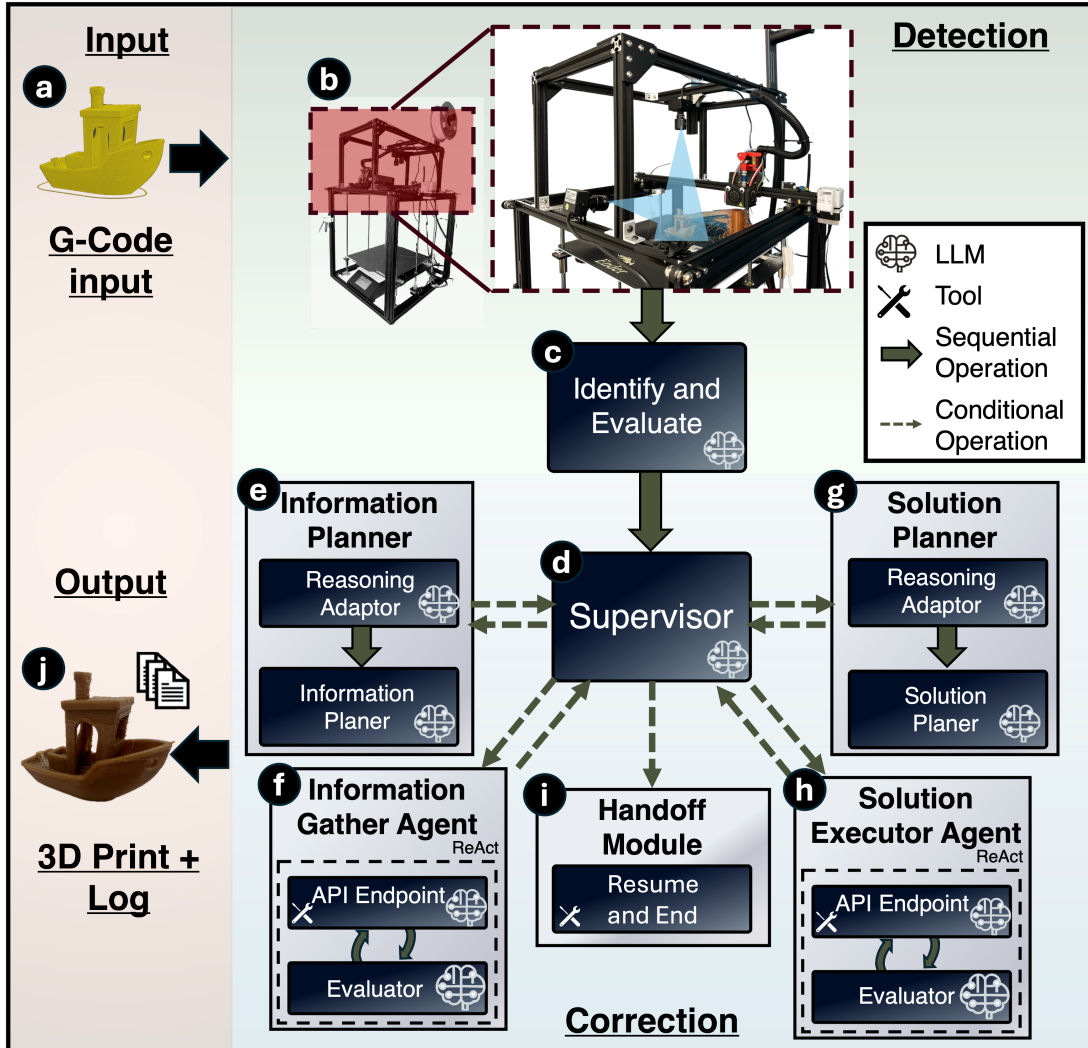


Figure 1: **Schematic of the Proposed Framework.** The process begins with a G-code file (a) being uploaded to the 3D printer, which is equipped with two frame-mounted cameras (b). After each layer is printed, the extruder moves to the home position, and two images of the current print state are captured (c). These images are analyzed by the LLM, which evaluates the print, makes observations, and identifies any failures. If failures are detected, the LLM supervisor (d) invokes the information planner (e). The executor (f) then carries out the information gathering plan, after which the solution planner (g) is activated by the supervisor. The solution plan is executed by another executor (h), and finally, the supervisor invokes the handoff module (j) to resume the print.

ongoing 3D print—one from the top and the other from the front once a layer is completed and the print is paused. These images, along with the description of the part, are fed into an LLM, which evaluates the print quality, identifies defects, and makes relevant observations.

Upon identifying an issue, the supervisory LLM invokes a planner to generate a detailed

plan outlining the necessary information and queries for the printer to diagnose the problem. Another LLM agent then executes tools to retrieve this information via the printer’s API. Based on the gathered data, the LLM generates a solution plan, which is implemented by another agent through direct communication with the printer’s API. After the solution is executed, the supervisory LLM verifies the parameters and resumes the print. The key advantage of this supervisory LLM is its ability to track the entire conversation among all LLM agents and orchestrate their actions as needed. This comprehensive oversight ensures system coordination and efficiency, with each agent being invoked precisely when necessary.

One of the significant benefits of this framework is its flexibility to work across various 3D printers, optimizing print parameters specific to each part without requiring any pre-existing dataset. This adaptability allows the system to fine-tune process parameters on-the-fly, accommodating different materials, geometries, and printer settings. Additionally, the LLM provides detailed process commentary, aiding in the certification of the part and enhancing traceability. This increases trust in the final product by comprehensively documenting the manufacturing process, reducing the need for destructive testing to validate part integrity. Real-time, insightful commentary on the printing process supports quality assurance and ensures compliance with industry standards and regulations.

Methodology

Given the complexity of the task, our multi-agent LLM framework consists of seven key modules, each designed to perform specific tasks independently as illustrated in Figure 1. The framework includes an Image-Based Reasoning Module (Figure 1c) that identifies defects and makes observations when the printer is paused. There are two planning modules, one focusing on gathering necessary information (Figure 1e) and the other on developing solutions to the identified issues (Figure 1g). Additionally, three execution modules interact directly with the 3D printer to apply these solutions (Figure 1f, h, i). A Supervisor Module

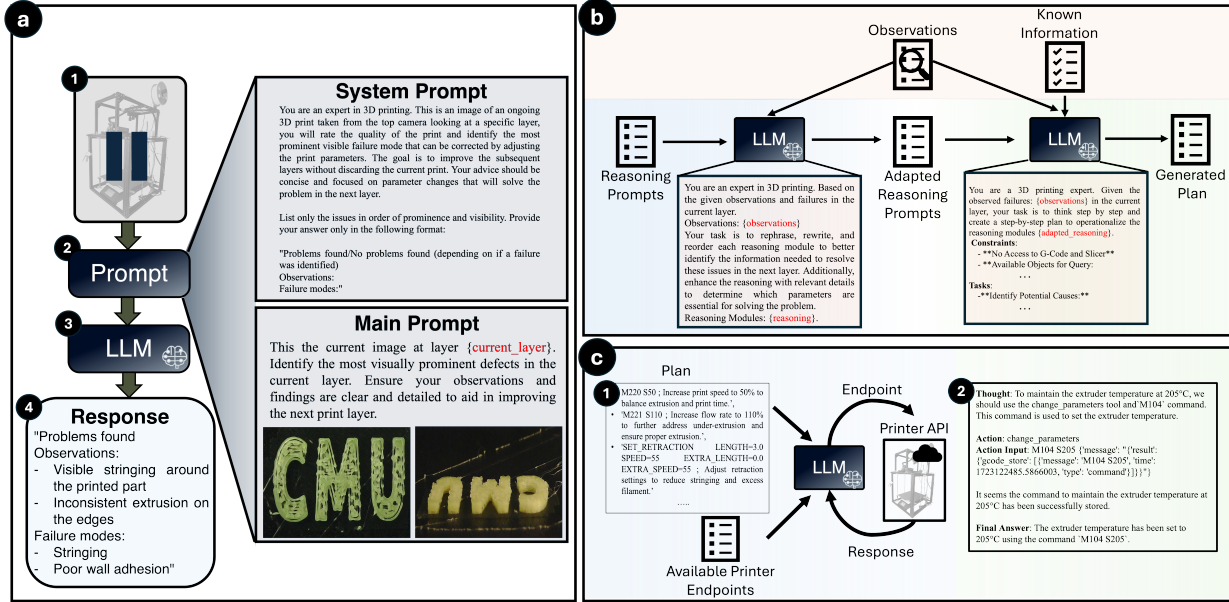


Figure 2: **Schematic of the Proposed Framework.** The process begins with a G-code file (a) being uploaded to the 3D printer, which is equipped with two frame-mounted cameras (b). After each layer is printed, the extruder moves to the home position, and two images of the current print state are captured (c). These images are analyzed by the LLM, which evaluates the print, makes observations, and identifies any failures. If failures are detected, the LLM supervisor (d) invokes the information planner (e). The executor (f) then carries out the information gathering plan, after which the solution planner (g) is activated by the supervisor. The solution plan is executed by another executor (h), and finally, the supervisor invokes the handoff module (j) to resume the print.

(Figure 1d) oversees the entire operation, maintaining a dynamic state dictionary that is accessible to other modules, facilitating agent communications, and orchestrating the timely activation of modules based on the current data and needs. By leveraging the specialized abilities and collaborative dynamics among these agents, our multi-agent system not only enhances efficiency in tackling complex tasks but also supports the integration of additional functionalities, allowing for scalable and adaptable enhancements as needed.

Error Detection

Large Vision-Language Models (LVLMs) such as MiniGPT-4¹⁰³ and LLaVA¹⁰⁴ have demonstrated significant capabilities in understanding and interpreting images, achieving remarkable performance across various visual tasks.^{105–108} Owing to extensive pre-training on large

datasets of image-text pairs, these models possess exceptional generalization abilities, enabling impressive zero-shot performance. They can effectively recognize and process both familiar and unfamiliar objects without the need for additional training data. This capability to generalize from diverse datasets makes them highly versatile and powerful tools for a wide range of visual and multimodal applications.

In this work, we leverage GPT-4o’s⁷⁷ image analysis capabilities to detect anomalies in ongoing 3D prints, enhancing the accuracy and reliability of the printing process by identifying and addressing issues in near real-time. After each layer is printed, the printer pauses, and two frame-mounted cameras capture images—one from the top (extruder view) and one from the front—after the extruder returns to its home position. These images along with a description of the part are fed into the LLM for analysis. To prevent redundant error identification, images from the last printed layer are also provided to the LLM, ensuring it does not detect previously addressed issues.

Our methodology employs a finely tuned prompt (SI 1) that instructs the LLM to act as a 3D printing expert agent. The LLM evaluates print quality, identifies visible failure modes, and provides structured, focused, and actionable responses in specified format.

Supervisor Agent

The Supervisor Agent plays a crucial role in orchestrating the interactions and activities of all modules within the system. It maintains a dynamic state dictionary (SI 4), where agents post updates and outputs from their interactions with the printer. This ensures that each module has access to the most current and relevant information before activation, optimizing the use of LLM tokens for maximum efficiency. As modules complete their assigned tasks, they update their status in the state dictionary. This allows the Supervisor Agent to effectively manage the sequence of module activations, ensuring smooth and efficient transitions between the various stages of the process.

Planning Agent

While LLMs have demonstrated emergent reasoning capabilities, their performance can be significantly enhanced when guided by a structured reasoning framework.^{109,110} Additionally, because the output of an LLM is heavily influenced by the quality and specificity of the prompts, it becomes essential to adapt these prompts based on the specific problems being addressed. Providing a well-defined reasoning structure and carefully tailored prompts allows the LLM to deliver more accurate and effective solutions, ensuring better outcomes for complex tasks.¹¹¹

To accomplish this, the planning agent (Fig 2) (b) is structured with two internal modules. The first module analyzes known information, observations and detected failures to select, adapt, and refine standard reasoning prompts (SI 2). This ensures that the planner works with the most optimized and relevant prompts when formulating a plan. The second module then leverages these tailored prompts and reasoning frameworks to develop a specific, actionable plan. This plan is carried out by the executor agents, which interact with the 3D printer via API to gather necessary data and implement the solution. This dual-module design enables the planning agent to effectively and efficiently resolve any issues that arise during

Executor Agent

The Agent Executor (Fig. 2c) , a crucial component of the framework, utilizes the ReAct (Reasoning and Acting) method¹¹² to execute the generated plans.

The Agent Executor uses a predefined Python function to communicate with the printer via its API. The process starts with the executor receiving a detailed plan from the planning agent, outlining specific actions and corresponding API endpoints. The executor then translates the plan into operational steps by calling these endpoints to run G-code scripts and available macros.

The ReAct method ensures that the executor is not simply issuing commands but actively

monitors printer responses and reasons through each step. After executing a command, the executor evaluates the 3D printer’s output. If the response is insufficient or indicates an incomplete action, the executor reassesses and adjusts by selecting an alternative endpoint or modifying the G-code script. This iterative approach continues until the desired outcome is achieved, ensuring accurate and efficient execution.

By continuously evaluating API outputs and adapting its actions based on real-time feedback, the Agent Executor effectively handles unforeseen issues and dynamically adjusts its approach.

Printer Setup

The printer setup consists of a consumer grade 3D printer modified to stream *in-situ* images and system information while also exposing an Application Program Interface (API) to accept commands to dynamically adjust printing parameters under the direction of an LLM agent. This is achieved with *Klipper*, an open source firmware project that delegates the task of parsing G-code and process monitoring away from the controller board to an external computer. *Klipper* in conjunction with ancillary plugins such as *Crowsnest*, *Moonraker*, and *Mainsail* provide a cohesive interface which allows for monitoring and control over various aspects of the printing process.

A stock *Crealitty Ender 5 Plus* 3D printer was reflashed with *Klipper* and configured alongside a standard desktop computer used as the host machine to deliver commands to the printer’s motor control unit. Two *SVPRO1080P* cameras with a 2.8 mm to 12 mm range of manual focus were placed to provide top and front views of the print (Fig. 1b). These cameras are configured with the *Crowsnext* plugin to stream images of the printing process from the host computer. Of the two cameras, the top one captures in-situ images of the printing process and these images are then provided as input to the multimodal LLM to identify and evaluate any defects in the ongoing print. An input image is captured using

with this camera at the specified end of a sequence of GCode commands. During the capture process the print is paused and toolhead is parked at home positions to avoid toolhead interference over the printed segment. These process parameter changes are made using the *Moonraker* API which exposes access to configurations such as the toolhead temperature, print speed, extrusion rate, or fan speed to name a few.

Result

We assessed the effectiveness of our framework on both multi-layer and single-layer 3D prints.

For the multi-layer prints, we conducted two primary experiments: one involving the printing of a spanner and the other featuring raised text, designed to simulate the complexities of multi-part prints. In these experiments, the optimization was done after the completion of each layer, allowing us to continuously monitor and optimize the printing process throughout the entire build.

To assess the effectiveness of the proposed framework at different sampling rates and its ability to identify and correct issues within a single layer, we conducted single-layer tests. These single-layer prints are particularly challenging yet crucial, as they establish the foundation for the entire print. For this analysis, we printed a 100mm x 100mm square with a height of 0.5mm, consisting of a single layer.

The single-layer print was divided into four distinct segments, each representing a different phase of the printing process. After completing each segment, an image was captured and analyzed by the LLM to identify potential failure modes. This analysis focused on detecting inconsistencies and errors through visual observations, providing insights into print quality at each stage. The objective was to determine how well the framework could maintain print integrity and correct issues within the foundational layer, which is critical for the success of the overall print.

Additionally, to evaluate the framework’s adaptability to different materials and its ability

to optimize parameters, we conducted tests using two different materials: PLA and TPU. Both prints were performed at a temperature of 190 °C, with the only variation being the print speed, which was set to 120 mm/s, and a layer height of 0.35mm. These tests aimed to verify the framework’s capability to work effectively across different materials and optimize parameters accordingly.

Multi Layer Prints

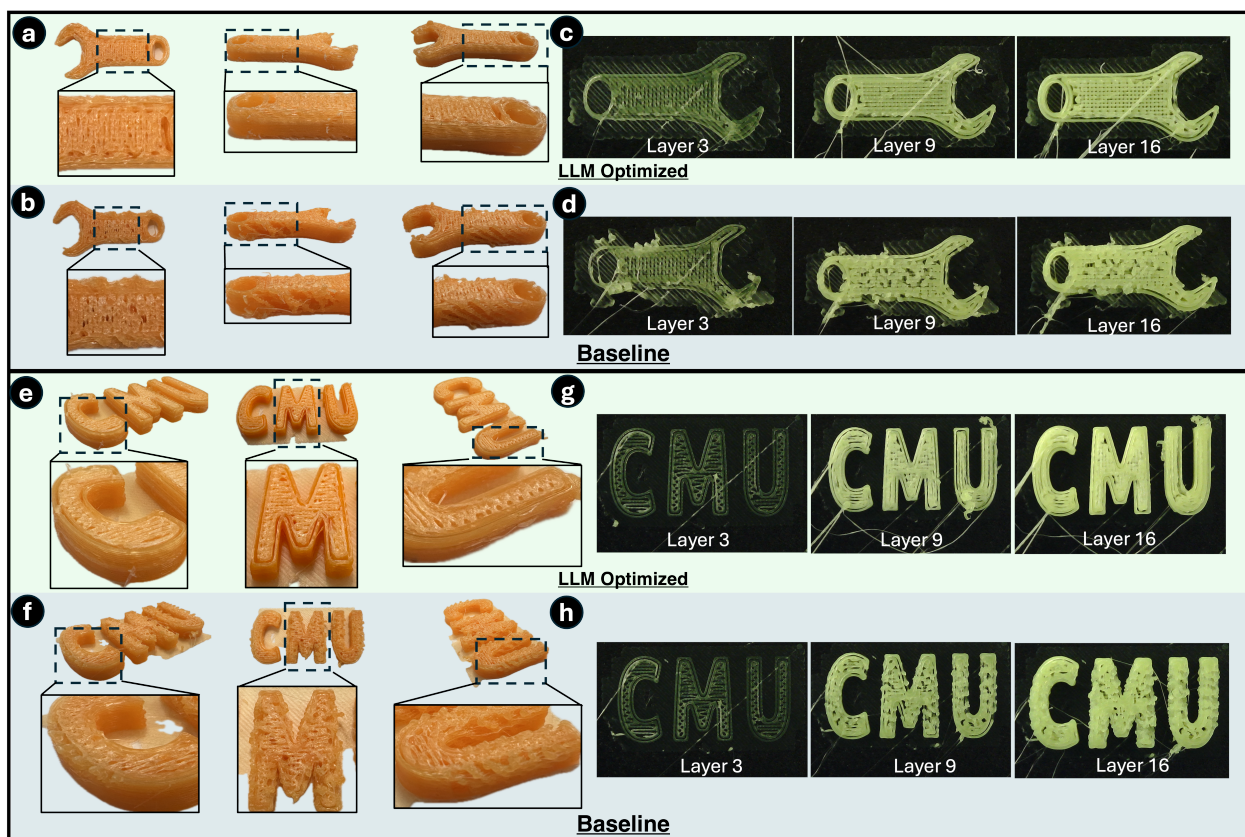


Figure 3: **Comparison of LLM-Optimized Print with Baseline:** (a) The LLM-optimized print exhibits cleaner, well-defined edges, while the baseline print shows (b) rough, uneven edges. (c) The LLM-optimized print maintains a consistently smooth surface finish, whereas the baseline print (d) displays rough surfaces with visible material deposition skips. (e) The LLM-optimized print demonstrates consistent extrusion and material deposition, in contrast to the baseline print (f), which suffers from uneven layer adhesion and under-extrusion. (g) The LLM-optimized prints show continuous improvements across layers, with better layer adhesion and more precise infill patterns, while the baseline prints display a steady deterioration in print quality.

To evaluate our framework’s ability to detect defects, correct printing errors, and optimize parameters, we used a 3D model of a wrench and raised text, sliced with a rectilinear infill pattern at 100% infill. Given that the framework requires pausing the print for error analysis and correction—a process that takes time—we added a 20mm diameter cylinder, matching the height of the wrench model, near the extruder’s homing position. This cylinder serves to purge oozed material during pauses and prime the nozzle when printing resumes. The toolpath was designed so that, after resuming, the printer first completes the corresponding layer of the cylinder before continuing with the main 3D model, ensuring smooth transitions and consistent print quality.

We selected PLA as the printing material, with the extruder temperature set to 200°C. Recognizing the critical importance of the first layer, default parameters were applied to ensure a solid foundation. For subsequent layers, the extrusion rate was reduced by 25%, and the print speed was set to 170 mm/s. These settings were chosen to fall within the standard range for PLA, providing a reliable baseline for successful printing while allowing the framework to effectively correct errors and optimize the printing process.

Additionally, for the print of the wrench model, a manual perturbation was introduced at Layer 10 to disrupt the correct Z-axis movement of the extruder, causing it to shift randomly. This was done to evaluate whether the LLM could accurately detect and respond to sudden, unexpected changes in the printing process. This disruption was not implemented programmatically through the printer’s API, as the LLM might have simply traced the last issued commands and recognized any intentional modifications to the Z-offset. By introducing a manual obstruction, the test aimed to challenge the LLM’s ability to identify and correct unplanned anomalies.

Figure 3 illustrates a comparison between 3D prints produced using a baseline approach and those optimized by the LLM, highlighting the substantial quality improvements achieved with LLM optimization. In Figure 3(a and b), the LLM-optimized print exhibits cleaner, well-defined edges, in contrast to the rough, uneven edges seen in the baseline print Figure

3(b and f). The surface finish also shows marked differences, with the LLM-optimized print maintaining a smooth, consistent texture, while the baseline print suffers from rough surfaces and skips in material deposition. Additionally, extrusion consistency is notably improved in the LLM-optimized print, which achieves uniform layer adhesion, whereas the baseline print is plagued by under-extrusion and poor layer bonding.

Additionally, layer-wise analysis in Figures 3(c and g) reveals continuous improvement in layer quality and infill patterns in the LLM-optimized prints, whereas the baseline prints (Figures 3(d and h)) deteriorate as the print progresses. The LLM-optimized approach not only addresses issues such as rough edges, inconsistent surfaces, and poor layer adhesion but also significantly enhances overall print quality, resulting in superior final products.

The stringing issue emerged as a result of the extruder pausing and moving to the home position during the print. The LLM worked to optimize the retraction settings to address this problem. However, despite these efforts, stringing remained unavoidable due to the combination of high flow rate, low print speed, and elevated temperature, which collectively exacerbate the issue. Although the LLM’s adjustments provided some improvement, these factors inherently make it challenging to completely eliminate stringing under the given conditions.

Parameter Optimization

To quantify the error/defect in single-layer prints, we define occupancy for each layer as:

$$occupancy = \frac{occupied_{pixels}}{total_{pixels}}$$

This metric provides a measure of how well the printed layer covers the intended area. For single-layer prints, the LLM identified several key parameters to adjust, including print speed, flow rate, pressure advance, and retraction flow for PLA prints, and nozzle temperature for TPU prints. Fig 4 illustrate the changes made by the LLM for single layer, with Figure 4a PLA print and Figure 4b TPU print. For print speed, the LLM suggested reducing it to 75%

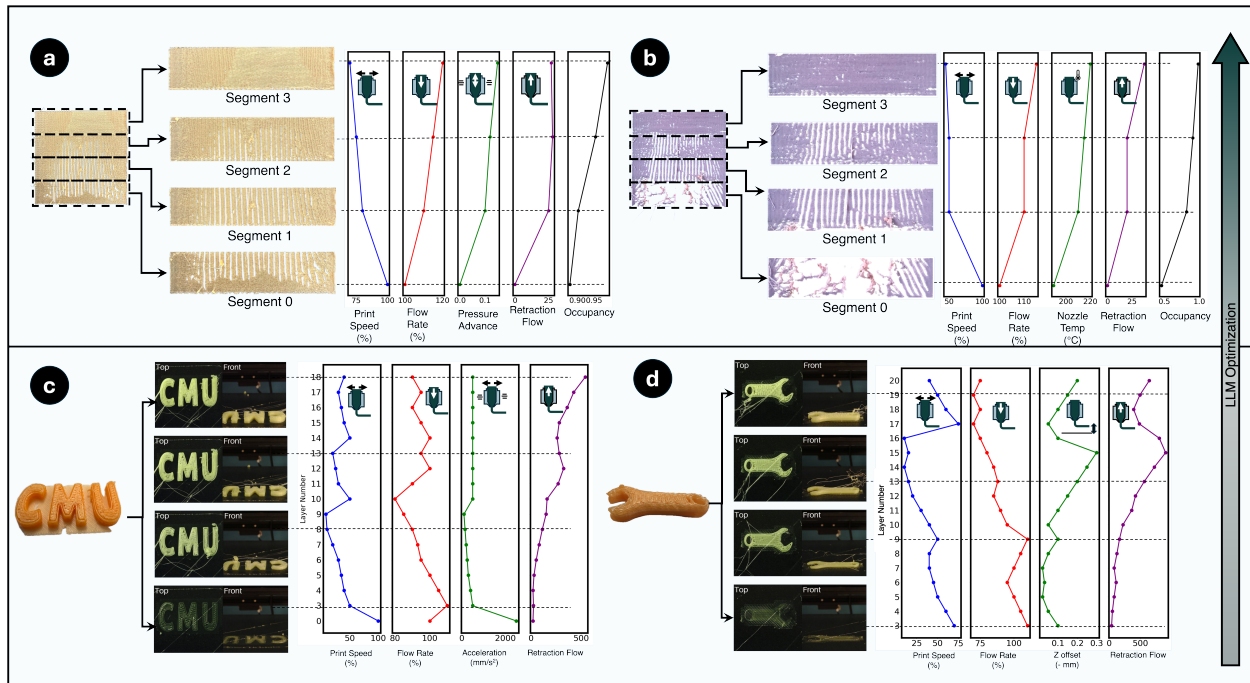


Figure 4: **LLM print parameter optimization** For single layer prints using (a) PLA, (b) TPU and for multi-layer prints of (c) text and (d) wrench.

to improve filament adhesion and minimize gaps. This change led to smoother deposition and more consistent layers. An adjustment to the flow rate, increasing it slightly above 100%, addressed the under-extrusion issues observed in the initial segments, resulting in a more uniform filament flow. A minor increase in pressure advance (up to 0.1) helped in managing the flow of filament, especially in corners and intricate details, reducing stringing and blobs. Optimizing retraction flow speed to around 25% mitigated the issues related to oozing and stringing between travel moves, enhancing the print's clean lines and precision. For TPU, the LLM suggested raising the nozzle temperature to 220°C, which improved filament melting and flow, leading to better layer adhesion and reduced stringing. The continuous increase in occupancy throughout the single-layer print, as shown, demonstrates the effectiveness of the LLM's optimization strategies in improving print quality.

The ability of the LLM to analyze and adjust parameters for different materials showcases its versatility. The images demonstrate that, following the LLM's recommendations, the quality of the prints improved significantly for both PLA and TPU. For PLA, the adjustments

led to smoother layers, better adhesion, and minimized gaps. For TPU, the optimized nozzle temperature and other parameter tweaks resulted in improved layer consistency and reduced stringing, common issues with flexible filaments.

For multi-layer print of wrench as illustrated in Figure 4 c, the LLM accurately identifies that the print speed and extrusion rate are off-nominal and actively seeks to optimize these parameters throughout the printing process. Additionally, despite the printer bed being correctly calibrated, the LLM continuously monitors the Z-axis position. Based on the provided layer height and the current layer number, the LLM adjusts the Z-offset of the printer to ensure a smooth surface finish. Notably, at Layer 10, the LLM detected that the Z position was misaligned and persistently attempted to correct it, demonstrating its capability to adapt and fine-tune the printing parameters.

For the print of raised text Figure 4d, the LLM initially identifies signs of under-extrusion and responds by increasing the flow rate, adjusting extruder acceleration, and reducing the print speed. These initial adjustments aim to stabilize the print quality and address the immediate under-extrusion issue. After these corrections, the LLM enters an optimization phase, where it systematically fine-tunes the print speed and flow rate to find the optimal settings for the specific print conditions.

This optimization process proves to be particularly effective in addressing stringing issues, as evidenced by the absence of stringing between the letters in the final print. The LLM's ability to dynamically adjust and optimize key parameters not only enhances the print quality but also demonstrates its capability to mitigate common issues like stringing, which are typically challenging to eliminate in complex prints like raised text.

Error Detection

Error detection is a vital element of the proposed framework. While LLMs are highly effective at analyzing textual data and sensor logs due to their advanced natural language processing capabilities, identifying subtle errors in a 3D print is challenging, especially when the model

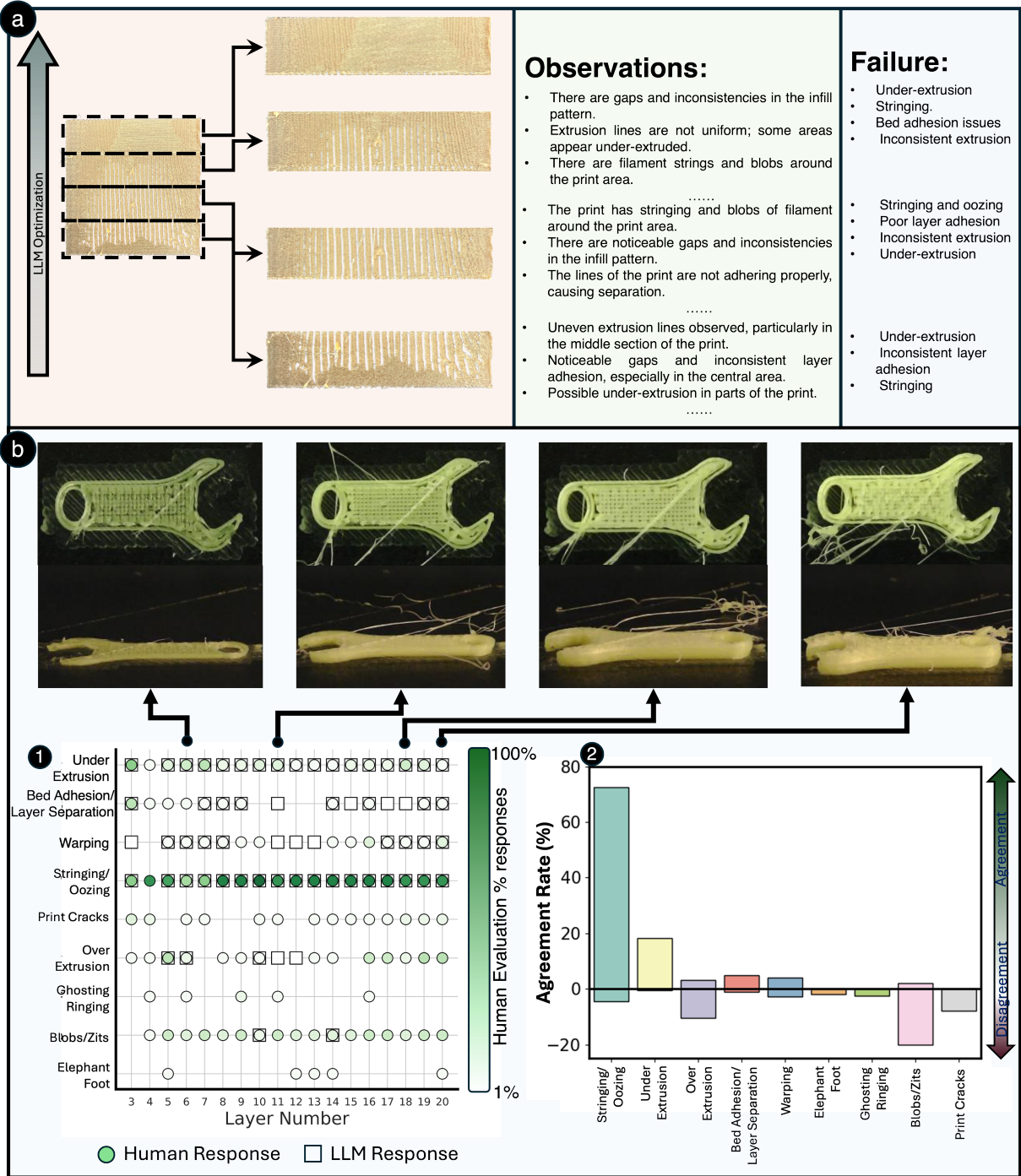


Figure 5: **Failures detected** (a) Observations and failures detected by the LLM in single-layer print during print optimization and for (b) Multi-Layer print of wrench. (b)(1) Comparison of collected human response and LLM response to multilayer print for each layer and (b)(2) the agreement score.

has not been specifically trained or fine-tuned on 3D printing data. To address this, we analyze the observations and errors detected by the LLM during the printing of a single layer.

The LLM accurately identified several key issues (Fig 5 a)at each segment of the print. It detected under-extrusion, nozzle clogs, inconsistent printing speeds, and bed leveling problems. These identifications were made by analyzing the visual characteristics of each segment’s print, such as gaps, stringing, and uneven filament deposition. From these observations, the LLM drew inferences about potential causes and provided recommendations for addressing the detected issues.

To demonstrate the effectiveness and error detection capability of the LLM (GPT-4o) in multi-layer prints, we conducted a comprehensive survey involving a diverse group of engineers, including graduate students with varying levels of experience in Additive Manufacturing (AM). The participants in this survey ranged from individuals with basic exposure to AM to those with advanced expertise in the field. Each participant was tasked with evaluating multi-layer 3D prints, specifically focusing on the prints that the LLM had analyzed and optimized during the printing process.

The participants were asked to identify major issues in the ongoing prints, such as layer adhesion, surface quality, and defects like under-extrusion, stringing, or warping. Their evaluations were then compared to the LLM’s automated detection and optimization process to determine how effectively the LLM identified and addressed these issues in real-time. This comparison allowed us to gauge not only the LLM’s accuracy in detecting and mitigating errors but also how its performance measured up against human expertise at various levels of experience.

To quantify the effectiveness of the LLM’s error detection relative to human evaluations, we introduce the metrics of agreement rate and disagreement rate. These metrics are defined as follows:

$$AgreementRate = \sum_i^N \frac{D_P}{Total_P} * D_{LLM}$$

$$DisagreementRate = - \sum_i^N \frac{D_P}{Total_P} * \hat{D}_{LLM}$$

Here, N represents the total number of layers in the print, D_P denotes the number of participants who identified a particular defect, and $Total_P$ is the total number of participants. D_{LLM} indicates whether the LLM detected the defect (initialized to 0 and set to 1 if the LLM identifies a defect), while \hat{D}_{LLM} represents defects not detected by the LLM (initialized to 1 and set to 0 if the LLM identifies the defect).

The agreement rate measures the alignment between the defects identified by the LLM and those recognized by the participants, reflecting the LLM’s accuracy in matching human observations. Conversely, the disagreement rate captures instances where the LLM failed to detect defects noted by participants, highlighting areas where the LLM’s performance may need improvement. These metrics provide a comprehensive assessment of the LLM’s ability to identify and correct printing defects compared to human evaluations.

Figure 5 b presents a comparison between participant responses and the LLM’s detection results. The analysis shows that both the LLM and the majority of participants consistently identified stringing (77%) and under-extrusion (55%) as significant issues across most print layers. Additionally, the LLM accurately detected more critical defects such as bed adhesion problems, warping, and layer separation.

The LLM did not detect some of the more subtle defects, such as print cracks, ghosting, ringing, and elephant foot, which were noted by approximately 1% of the participants. This discrepancy could be due to the resolution limitations of the camera used for image capture, which may not have been sufficient to detect these finer details. Another possibility is that these minor issues were misidentified by the participant evaluators, resulting in a difference between human and LLM detection.

Interestingly, the LLM successfully identified blobs and zits in layers 10 and 15, but it

attributed these issues to stringing and oozing defects in other layers. This suggests that while the LLM is effective at detecting and categorizing certain types of defects, it may occasionally generalize or misclassify closely related issues, particularly when dealing with subtle variations in print quality. This highlights both the LLM’s strengths in detecting major defects and areas where further refinement is needed to improve its sensitivity to minor or less common issues.

Based on the agreement-disagreement scores, it can be observed that the LLM and human evaluators show a 77% agreement on identifying stringing/oozing defects, a 20% agreement on under-extrusion, and a 7% agreement on over-extrusion. Additionally, there is a maximum of 20% disagreement between the LLM and humans for blobs and zits defect. These figures indicate that the LLM demonstrates strong alignment with human assessments for key visual defects like stringing/oozing and inconsistent extrusion. The close agreement on critical defects shows the LLM’s potential, with room for growth in more nuanced areas.

Conclusion

We developed and tested a framework using GPT-4o to detect and address 3D printing defects in near real-time. The LLM effectively identifies major defects like stringing, oozing, layer separation, and inconsistent extrusion, closely matching human evaluations. By dynamically adjusting print parameters based on real-time analysis, the framework significantly enhances print quality and reduces material waste.

A key strength of the LLM framework is its ability to not only detect defects but also to identify the underlying parameters causing these issues. Upon recognizing a defect, the LLM analyzes related print parameters, such as print speed, flow rate, temperature, and retraction settings, to determine their contribution to the problem. It then initiates an optimization process, adjusting these parameters to correct the detected issues in subsequent layers. This proactive approach allows for continuous improvement of the print quality, minimizing the

likelihood of defects recurring and enhancing the overall efficiency of the printing process. The agreement-disagreement analysis between the LLM and human evaluators highlights both the strengths and opportunities for further development. The high agreement rates on key defects underscore the LLM’s effectiveness.

An important aspect of this framework is its ability to generate detailed manufacturing commentary and defect detection reports, which significantly enhance part defect traceability and automated documentation. By providing a comprehensive log of the issues encountered and the adjustments made during the printing process, the LLM facilitates better tracking of part quality from start to finish. This automated documentation not only aids in identifying the root causes of defects but also streamlines quality control processes, making it easier to certify parts for use in critical applications and ensuring compliance with industry standards.

Overall, the integration of LLMs into the 3D printing process represents a promising advancement in additive manufacturing. As these models continue to evolve, their ability to detect and correct a broader range of defects will likely improve, making them invaluable tools in achieving higher precision and reliability in AM.

References

- (1) Xu, L. D.; Xu, E. L.; Li, L. Industry 4.0: state of the art and future trends. *International journal of production research* **2018**, *56*, 2941–2962.
- (2) Gunal, M. M. Simulation and the fourth industrial revolution. *Simulation for Industry 4.0: Past, Present, and Future* **2019**, 1–17.
- (3) Pascoal-Faria, P.; da Silva, D. P.; Mateus, A.; Mitchell, G. R. Digitalisation of material science—Improving product design in the context of Industry 4.0. *Materials Today: Proceedings* **2023**,
- (4) Bauza, M.; Tenboer, J.; Li, M.; Lisovich, A.; Zhou, J.; Pratt, D. S.; Edwards, J.;

- Zhang, H.; Turch, C.; Knebel, R. Realization of Industry 4.0 with high speed CT in high volume production. *CIRP Journal of Manufacturing Science and Technology* **2018**,
- (5) Wang, W.; Niu, N.; Alenazi, M.; Xu, L. D. In-Place Traceability for Automated Production Systems: A Survey of PLC and SysML Tools. *IEEE Transactions on Industrial Informatics* **2019**, *15*, 3155–3162.
- (6) Yadroitsev, I.; Yadroitsava, I.; Du Plessis, A.; MacDonald, E. *Fundamentals of laser powder bed fusion of metals*; Elsevier, 2021.
- (7) Jin, Z.; Zhang, Z.; Demir, K. G.; Gu, G. X. Machine Learning for Advanced Additive Manufacturing. **2020**, *3*, 1541–1556.
- (8) Faludi, J.; Bayley, C.; Bhogal, S.; Iribarne, M. Comparing environmental impacts of additive manufacturing vs traditional machining via life-cycle assessment. *Rapid Prototyping Journal* **2015**, *21*, 14–33.
- (9) Buj-Corral, I.; Tejo-Otero, A.; Fenollosa-Artés, F. Use of FDM technology in health-care applications: recent advances. *Fused Deposition Modeling Based 3D Printing* **2021**, 277–297.
- (10) Giannatsis, J.; Dedoussis, V. Additive fabrication technologies applied to medicine and health care: a review. *The International Journal of Advanced Manufacturing Technology* **2009**, *40*, 116–127.
- (11) da Silva, L. R. R.; Sales, W. F.; Campos, F. d. A. R.; de Sousa, J. A. G.; Davis, R.; Singh, A.; Coelho, R. T.; Borgohain, B. A comprehensive review on additive manufacturing of medical devices. *Progress in Additive Manufacturing* **2021**, *6*, 517–553.
- (12) Haghighashtiani, G.; Qiu, K.; Zhingre Sanchez, J. D.; Fuenning, Z. J.; Nair, P.; Ahlberg, S. E.; Iaizzo, P. A.; McAlpine, M. C. 3D printed patient-specific aortic root

- models with internal sensors for minimally invasive applications. *Science advances* **2020**, *6*, eabb4641.
- (13) Najmon, J. C.; Raeisi, S.; Tovar, A. Review of additive manufacturing technologies and applications in the aerospace industry. *Additive manufacturing for the aerospace industry* **2019**, 7–31.
- (14) Stano, G.; Percoco, G. Additive manufacturing aimed to soft robots fabrication: A review. *Extreme Mechanics Letters* **2021**, *42*, 101079.
- (15) O’Neill, P. F.; Ben Azouz, A.; Vazquez, M.; Liu, J.; Marczak, S.; Slouka, Z.; Chang, H. C.; Diamond, D.; Brabazon, D. Advances in three-dimensional rapid prototyping of microfluidic devices for biological applications. *Biomicrofluidics* **2014**, *8*.
- (16) Bacciaglia, A.; Ceruti, A.; Liverani, A. Evaluation of 3D printed mouthpieces for musical instruments. *Rapid Prototyping Journal* **2020**, *26*, 577–584.
- (17) Gibson, I.; Rosen, D. W.; Stucker, B.; Khorasani, M.; Rosen, D.; Stucker, B.; Khorasani, M. *Additive manufacturing technologies*; Springer, 2021; Vol. 17.
- (18) Sells, E.; Bailard, S.; Smith, Z.; Bowyer, A.; Olliver, V. *Handbook of Research in Mass Customization and Personalization: (In 2 Volumes)*; World Scientific, 2010; pp 568–580.
- (19) Jones, R.; Haufe, P.; Sells, E.; Iravani, P.; Olliver, V.; Palmer, C.; Bowyer, A. RepRap—the replicating rapid prototyper. *Robotica* **2011**, *29*, 177–191.
- (20) Laplume, A.; Anzalone, G. C.; Pearce, J. M. Open-source, self-replicating 3-D printer factory for small-business manufacturing. *The International Journal of Advanced Manufacturing Technology* **2016**, *85*, 633–642.
- (21) Pearce, J. M. Building research equipment with free, open-source hardware. *Science* **2012**, *337*, 1303–1304.

- (22) Pearce, J. M. *Open-source lab: how to build your own hardware and reduce research costs*; Newnes, 2013.
- (23) Peng, A.; Xiao, X. Investigation on reasons inducing error and measures improving accuracy in fused deposition modeling. *Advances in Information Sciences and Service Sciences* **2012**, *4*.
- (24) Agarwala, M. K.; Jamalabad, V. R.; Langrana, N. A.; Safari, A.; Whalen, P. J.; Danforth, S. C. Structural quality of parts processed by fused deposition. *Rapid prototyping journal* **1996**, *2*, 4–19.
- (25) Hsiang Loh, G.; Pei, E.; Gonzalez-Gutierrez, J.; Monzón, M. An overview of material extrusion troubleshooting. *Applied Sciences* **2020**, *10*, 4776.
- (26) All3DP Common 3D Printing Problems: Troubleshooting 3D Printer Issues. <https://all3dp.com/1/common-3d-printing-problems-troubleshooting-3d-printer-issues/>, n.d.; Accessed: 2024-06-25.
- (27) Nuchitprasitchai, S.; Roggemann, M.; Pearce, J. M. Factors effecting real-time optical monitoring of fused filament 3D printing. *Progress in Additive Manufacturing* **2017**, *2*, 133–149.
- (28) Samykano, M.; Selvamani, S. K.; Kadirgama, K.; Ngui, W. K.; Kanagaraj, G.; Sudhakar, K. Mechanical property of FDM printed ABS: influence of printing parameters. *The International Journal of Advanced Manufacturing Technology* **2019**, *102*, 2779–2796.
- (29) Song, R.; Telenko, C. Causes of Desktop FDM Fabrication Failures in an Open Studio Environment. *Procedia CIRP* **2019**,

- (30) Dey, A.; Yodo, N. A Systematic Survey of FDM Process Parameter Optimization and Their Influence on Part Characteristics. *Journal of Manufacturing and Materials Processing* **2019**,
- (31) Baraheni, M.; Shabgard, M. R.; Tabatabaee, A. M. Effects of FDM 3D printing parameters on PLA biomaterial components dimensional accuracy and surface quality. *Proceedings of the Institution of Mechanical Engineers, Part C: Journal of Mechanical Engineering Science* **2023**,
- (32) Wittbrodt, B. T.; Glover, A. G.; Laureto, J.; Anzalone, G.; Oppliger, D.; Irwin, J.; Pearce, J. M. Life-cycle economic analysis of distributed manufacturing with open-source 3-D printers. *Mechatronics* **2013**, *23*, 713–726.
- (33) Song, R.; Telenko, C. Material and energy loss due to human and machine error in commercial FDM printers. *Journal of cleaner production* **2017**, *148*, 895–904.
- (34) Garzon-Hernandez, S.; Garcia-Gonzalez, D.; Jérusalem, A.; Arias, A. Design of FDM 3D printed polymers: An experimental-modelling methodology for the prediction of mechanical properties. *Materials & Design* **2020**,
- (35) Wu, H.; Wang, Y.; Yu, Z. In situ monitoring of FDM machine condition via acoustic emission. *The International Journal of Advanced Manufacturing Technology* **2015**, *84*, 1483–1495.
- (36) Caltanissetta, F.; Dreifus, G.; Hart, A. J.; Colosimo, B. M. In-situ monitoring of material extrusion processes via thermal videoimaging with application to big area additive manufacturing (baam). *Additive Manufacturing* **2022**, *58*, 102995.
- (37) Duan, M.; Chen, S.; Yang, Y. Thermal-image-enabled additive manufacturing process monitoring and extrusion trajectory compensation. International Manufacturing Science and Engineering Conference. 2023; p V001T01A018.

- (38) Oleff, A.; Küster, B.; Stonis, M.; Overmeyer, L. Process monitoring for material extrusion additive manufacturing: a state-of-the-art review. *Progress in Additive Manufacturing* **2021**, *6*, 705–730.
- (39) Fu, Y.; Downey, A.; Yuan, L.; Pratt, A.; Balogun, Y. In situ monitoring for fused filament fabrication process: A review. *Additive Manufacturing* **2021**, *38*, 101749.
- (40) Li, Y.; Zhao, W.; Li, Q.; Wang, T.; Wang, G. In-situ monitoring and diagnosing for fused filament fabrication process based on vibration sensors. *Sensors* **2019**, *19*, 2589.
- (41) Liu, J.; Hu, Y.; Wu, B.; Wang, Y. An improved fault diagnosis approach for FDM process with acoustic emission. *Journal of Manufacturing Processes* **2018**, *35*, 570–579.
- (42) Li, Z.; Zhang, Z.; Shi, J.; Wu, D. Prediction of surface roughness in extrusion-based additive manufacturing with machine learning. *Robotics and Computer-Integrated Manufacturing* **2019**, *57*, 488–495.
- (43) Bhavsar, P.; Sharma, B.; Moscoso-Kingsley, W.; Madhavan, V. Detecting first layer bond quality during FDM 3D printing using a discrete wavelet energy approach. *Procedia Manufacturing* **2020**, *48*, 718–724.
- (44) Faes, M.; Abbeloos, W.; Vogeler, F.; Valkenaers, H.; Coppens, K.; Goedemé, T.; Ferraris, E. Process monitoring of extrusion based 3D printing via laser scanning. *arXiv preprint arXiv:1612.02219* **2016**,
- (45) Brion, D. A.; Pattinson, S. W. Generalisable 3D printing error detection and correction via multi-head neural networks. *Nature communications* **2022**, *13*, 4654.
- (46) Baumann, F.; Roller, D. Vision based error detection for 3D printing processes. MATEC web of conferences. 2016; p 06003.

- (47) Moretti, M.; Bianchi, F.; Senin, N. Towards the development of a smart fused filament fabrication system using multi-sensor data fusion for in-process monitoring. *Rapid prototyping journal* **2020**, *26*, 1249–1261.
- (48) Cheng, Y.; Jafari, M. A. Vision-based online process control in manufacturing applications. *IEEE Transactions on Automation Science and Engineering* **2008**, *5*, 140–153.
- (49) He, K.; Zhang, Q.; Hong, Y. Profile monitoring based quality control method for fused deposition modeling process. *Journal of Intelligent Manufacturing* **2019**, *30*, 947–958.
- (50) Costa, S.; Duarte, F.; Covas, J. Estimation of filament temperature and adhesion development in fused deposition techniques. *Journal of Materials Processing Technology* **2017**, *245*, 167–179.
- (51) Dinwiddie, R. B.; Love, L. J.; Rowe, J. C. Real-time process monitoring and temperature mapping of a 3D polymer printing process. *Thermosense: Thermal Infrared Applications XXXV*. 2013; pp 165–173.
- (52) Holzmond, O.; Li, X. In situ real time defect detection of 3D printed parts. *Additive Manufacturing* **2017**, *17*, 135–142.
- (53) Fastowicz, J.; Grudziński, M.; Teclaw, M.; Okarma, K. Objective 3D printed surface quality assessment based on entropy of depth maps. *Entropy* **2019**, *21*, 97.
- (54) Liu, C.; Law, A. C. C.; Roberson, D.; Kong, Z. Image analysis-based closed loop quality control for additive manufacturing with fused filament fabrication. *Journal of Manufacturing Systems* **2019**, *51*, 75–86.
- (55) Jadhav, Y.; Berthel, J.; Hu, C.; Panat, R.; Beuth, J.; Farimani, A. B. StressD: 2D Stress estimation using denoising diffusion model. *Computer Methods in Applied Mechanics and Engineering* **2023**, *416*, 116343.

- (56) Ogoke, F.; Liu, Q.; Ajenifujah, O.; Myers, A.; Quirarte, G.; Beuth, J.; Malen, J.; Farimani, A. B. Inexpensive High Fidelity Melt Pool Models in Additive Manufacturing Using Generative Deep Diffusion. *arXiv preprint arXiv:2311.16168* **2023**,
- (57) Ogoke, F.; Pak, P. M.-W.; Myers, A.; Quirarte, G.; Beuth, J.; Malen, J.; Farimani, A. B. Deep Learning for Melt Pool Depth Contour Prediction From Surface Thermal Images via Vision Transformers. *arXiv preprint arXiv:2404.17699* **2024**,
- (58) Strayer, S. T.; Templeton, W. J. F.; Dugast, F. X.; Narra, S. P.; To, A. C. Accelerating High-Fidelity Thermal Process Simulation of Laser Powder Bed Fusion via the Computational Fluid Dynamics Imposed Finite Element Method (CIFEM). *Additive Manufacturing Letters* **2022**, *3*, 100081.
- (59) Jadhav, Y.; Berthel, J.; Hu, C.; Panat, R.; Beuth, J.; Farimani, A. B. Generative Lattice Units with 3D Diffusion for Inverse Design: GLU3D. *Advanced Functional Materials* **2024**,
- (60) Pak, P. M.-W.; Ogoke, F.; Polonsky, A.; Garland, A.; Bolintineanu, D. S.; Moser, D. R.; Heiden, M. J.; Farimani, A. B. ThermoPore: Predicting Part Porosity Based on Thermal Images Using Deep Learning. *arXiv preprint arXiv:2404.16882* **2024**,
- (61) Tian, Q.; Tian, Q.; Guo, S.; Melder, E.; Bian, L.; Guo, W. Deep Learning-Based Data Fusion Method for In Situ Porosity Detection in Laser-Based Additive Manufacturing. *Journal of Manufacturing Science and Engineering* **2020**,
- (62) Taherkhani, K.; Eischer, C.; Toyserkani, E. An unsupervised machine learning algorithm for in-situ defect-detection in laser powder-bed fusion. *Journal of Manufacturing Processes* **2022**, *81*, 476–489.
- (63) Cao, Z.; Farimani, O. B.; Ock, J.; Farimani, A. B. Machine Learning in Membrane Design: From Property Prediction to AI-Guided Optimization. *Nano letters*

- (64) Ajenifujah, O. T.; Ogoke, F.; Wirth, F.; Beuth, J.; Farimani, A. B. Integrating Multi-Physics Simulations and Machine Learning to Define the Spatter Mechanism and Process Window in Laser Powder Bed Fusion. *arXiv preprint arXiv:2405.07823* **2024**,
- (65) Jin, Z.; Zhang, Z.; Gu, G. X. Autonomous in-situ correction of fused deposition modeling printers using computer vision and deep learning. *Manufacturing Letters* **2019**, *22*, 11–15.
- (66) Saluja, A.; Xie, J.; Fayazbakhsh, K. A closed-loop in-process warping detection system for fused filament fabrication using convolutional neural networks. *Journal of Manufacturing Processes* **2020**, *58*, 407–415.
- (67) Delli, U.; Chang, S. Automated process monitoring in 3D printing using supervised machine learning. *Procedia Manufacturing* **2018**, *26*, 865–870.
- (68) Jin, Z.; Zhang, Z.; Gu, G. X. Automated real-time detection and prediction of interlayer imperfections in additive manufacturing processes using artificial intelligence. *Advanced Intelligent Systems* **2020**, *2*, 1900130.
- (69) Brion, D. a. J.; Pattinson, S. W. Generalisable 3D printing error detection and correction via multi-head neural networks. *Nature Communications* **2022**, *13*.
- (70) Vaswani, A.; Shazeer, N.; Parmar, N.; Uszkoreit, J.; Jones, L.; Gomez, A. N.; Kaiser, L.; Polosukhin, I. Attention is all you need. *Advances in neural information processing systems*. 2017; pp 5998–6008.
- (71) Lin, Z.; Gan, Z.; Han, S.; Liu, Z.; Sun, M.; He, J.; Zhao, C.; Liu, Z. A survey of transformers. *arXiv preprint arXiv:2106.04554* **2022**,
- (72) Brown, T. B.; Mann, B.; Ryder, N.; Subbiah, M.; Kaplan, J. D.; Dhariwal, P.; Nee-lakantan, A.; Shyam, P.; Sastry, G.; Askell, A.; others Language models are few-shot learners. *Advances in neural information processing systems*. 2020; pp 1877–1901.

- (73) Chowdhery, A.; Narang, S.; Devlin, J.; Bosma, M.; Mishra, G.; Roberts, A.; Barham, P.; Chung, H. W.; Sutton, C.; Gehrmann, S.; others PaLM: Scaling language modeling with pathways. *arXiv preprint arXiv:2204.02311* **2023**,
- (74) Chung, H. W.; Hou, L.; Longpre, S.; Zoph, B.; Tay, Y.; Fedus, L.; Li, E.; Wang, X.; Dehghani, M.; Brahma, S.; others Scaling instruction-finetuned language models. *arXiv preprint arXiv:2210.11416* **2022**,
- (75) Chang, J. H.; Singh, V.; Harer, J.; Varshney, L. R. A survey on instruction-tuned language models. *arXiv preprint arXiv:2304.08469* **2023**,
- (76) Zhao, W.; Zhang, W.; Zhao, Y.; Zhang, Z. A survey on large language models. *arXiv preprint arXiv:2303.18223* **2023**,
- (77) Achiam, J.; Leike, J.; McGrew, B.; Irving, G.; Amodei, D.; Brockman, G.; Sutskever, I.; Clark, J.; Engstrom, L. GPT-4: OpenAI’s Most Advanced System. *arXiv preprint arXiv:2303.14410* **2023**,
- (78) Zhou, K.; Ghosh, S.; Xie, S.; Narang, S.; Fedus, L.; Li, E.; Dean, J. Instruction-Following Models. *arXiv preprint arXiv:2302.10274* **2023**,
- (79) Wang, Y.; Kordi, Y.; Mishra, S.; Liu, A.; Smith, N. A.; Hajishirzi, H. Self-Instruct: Aligning Language Models with Self Generated Instructions. *arXiv preprint arXiv:2212.10560* **2022**,
- (80) Webb, S.; Palen-Michel, C.; Liu, A.; Wei, J.; Tworek, J. Emergent Properties of Finetuned Language Models. *arXiv preprint arXiv:2211.15664* **2022**,
- (81) Huang, H.; Zha, S.; Chen, Z.; Li, T.; Zhao, D.; Dong, Y. Towards Reasoning in Large Language Models: A Survey. *arXiv preprint arXiv:2212.11692* **2022**,
- (82) Lin, Z.; Liu, Q.; Xu, Z.; Chen, F. Few-shot Learning with Language Models: A Survey. *arXiv preprint arXiv:2105.11447* **2021**,

- (83) Perez, E.; Johnson, M.; Goodman, N.; Kim, D. True Few-shot Learning with Language Models. *arXiv preprint arXiv:2105.11447* **2021**,
- (84) Boiko, D. A.; MacKnight, R.; Gomes, G. Emergent autonomous scientific research capabilities of large language models. *ArXiv* **2023**, *abs/2304.05332*.
- (85) Bran, A.; Teera, V.; Jensen, J. ChemCrow: Augmenting large-language models with chemistry tools. *ArXiv* **2023**,
- (86) Romera-Paredes, B.; Ball, P.; Lampert, C.; others Mathematical capabilities of large language models. *ArXiv* **2024**,
- (87) Thapa, R.; Anik, R.; Basnet, B.; others ChatGPT’s potential in biomedical research. *BioMed Central* **2023**,
- (88) Chen, Y.; Zhao, H.; Lin, X.; others Extensive evaluation of ChatGPT for drug discovery and biomedical applications. *ArXiv* **2023**,
- (89) Lee, J.; Yoon, W.; Kim, S.; others BioBERT: a pre-trained biomedical language representation model for biomedical text mining. *Bioinformatics* **2020**, *36*, 1234–1240.
- (90) Zaki, M.; Fu, Y.; Xing, J.; others MAScQA: Materials Science Question Answering. *ArXiv* **2023**,
- (91) Xie, T.; Dai, H.; others Large language models for materials science: Recent advances and future directions. *ArXiv* **2023**,
- (92) Zhu, Z.; Lin, Z.; Wang, S.; others ChatGPT for environmental science: Opportunities and challenges. *ArXiv* **2023**,
- (93) Holmes, D.; Thomas, P.; others Evaluating large language models in the scientific domain. *ArXiv* **2023**,

- (94) Qin, Y.; Xiao, L.; others ChatGPT in science: Opportunities, challenges, and implications. *ArXiv* **2023**,
- (95) Zeng, Y.; Wang, Q.; others Large language models in scientific research: A comprehensive survey. *ArXiv* **2023**,
- (96) Wang, X.; Shi, Y.; others Voyager: An autonomous agent for scientific discovery. *ArXiv* **2023**,
- (97) Bartsch, A.; Farimani, A. B. LLM-Craft: Robotic Crafting of Elasto-Plastic Objects with Large Language Models. *arXiv preprint arXiv:2406.08648* **2024**,
- (98) Yang, F.; Wang, J.; others Large language models as versatile optimizers. *ArXiv* **2023**,
- (99) Buehler, M. J. MechGPT, a language-based strategy for mechanics and materials modeling that connects knowledge across scales, disciplines and modalities. *ArXiv* **2023**, *abs/2310.10445*.
- (100) Chandrasekhar, A.; Chan, J.; Ogoke, F.; Ajenifujah, O.; Farimani, A. B. AMGPT: a Large Language Model for Contextual Querying in Additive Manufacturing. *arXiv preprint arXiv:2406.00031* **2024**,
- (101) Picard, C.; Bourgeois, R.; others Concept generation through sketch similarity analysis using large language models. *ArXiv* **2023**,
- (102) Jadhav, Y.; Farimani, A. B. Large language model agent as a mechanical designer. *arXiv preprint arXiv:2404.17525* **2024**,
- (103) Zhu, D.; Chen, J.; Shen, X.; Li, X.; Elhoseiny, M. Minigpt-4: Enhancing vision-language understanding with advanced large language models. *arXiv preprint arXiv:2304.10592* **2023**,
- (104) Liu, H.; Li, C.; Wu, Q.; Lee, Y. J. Visual instruction tuning. *Advances in neural information processing systems* **2024**, *36*.

- (105) Cao, Y.; Xu, X.; Sun, C.; Cheng, Y.; Du, Z.; Gao, L.; Shen, W. Segment Any Anomaly without Training via Hybrid Prompt Regularization. *arXiv.org* **2023**,
- (106) Zhu, J.; Cai, S.; Deng, F.; Wu, J. Do llms understand visual anomalies? uncovering llm capabilities in zero-shot anomaly detection. *arXiv preprint arXiv:2404.09654* **2024**,
- (107) Elhafsi, A.; Sinha, R.; Agia, C.; Schmerling, E.; Nesnas, I. A.; Pavone, M. Semantic anomaly detection with large language models. *Autonomous Robots* **2023**, *47*, 1035–1055.
- (108) Gu, Z.; Zhu, B.; Zhu, G.; Chen, Y.; Tang, M.; Wang, J. Anomalygpt: Detecting industrial anomalies using large vision-language models. Proceedings of the AAAI Conference on Artificial Intelligence. 2024; pp 1932–1940.
- (109) Moghaddam, S. R.; Honey, C. Boosting Theory-of-Mind Performance in Large Language Models via Prompting. *ArXiv* **2023**, *abs/2304.11490*.
- (110) Zhang, H.; Cai, M.; Zhang, X.; Zhang, C. J.; Mao, R.; Wu, K. Self-Convinced Prompting: Few-Shot Question Answering with Repeated Introspection. *ArXiv* **2023**, *abs/2310.05035*.
- (111) Significant-Gravitas GitHub - Significant-Gravitas/AutoGPT: AutoGPT is the vision of accessible AI for everyone, to use and to build on. Our mission is to provide the tools, so that you can focus on what matters. <https://github.com/Significant-Gravitas/AutoGPT>.
- (112) Sivarakumar, S.; Kelley, M.; Samolyk-Mazzanti, A.; Visweswaran, S.; Wang, Y. An Empirical Evaluation of Prompting Strategies for Large Language Models in Zero-Shot Clinical Natural Language Processing. *ArXiv* **2023**, *abs/2309.08008*.